Supplementary information

Physico-chemical characterization of ferrocifen lipid nanocapsules: customized drug delivery systems guided by the molecular structure

Pierre Idlas[1], Elise Lepeltier[1,*], Guillaume Bastiat[1], Pascal Pigeon[2,3], Michael J. McGlinchey[4], Nolwenn Lautram[1], Anne Vessières[2], Gerard Jaouen[2,3] and Catherine Passirani[1]

[1] Micro et Nanomédecines Translationnelles, MINT, UNIV Angers, INSERM 1066, CNRS 6021, Angers, France`

[2] Sorbonne Université, CNRS, Institut Parisien de Chimie Moléculaire (IPCM), 75005 Paris, France

[3] Chimie Paris Tech, PSL University, 75005 Paris, France

[4] UCD School of Chemistry, University College Dublin, Belfield, Dublin 4, Ireland

* Corresponding author: elise.lepeltier@univ-angers.fr

EXPERIMENTAL SECTION (Supplementary information)

Solubility study in caprylic/capric triglycerides (Labrafac® WL 1349). Solubility of **P722**, **P769**, the two isomers of **P849** and the two isomers of **P998** was determined as followed: excess amount of ferrocifen were added in vial containing Labrafac® WL 1349. The mixture was put under stirring in water bath heated at 60°C for 90 min. Subsequently, the mixture was then centrifuged at 1,400 g for 5 min. Finally, the supernatant concentration was determined using UPLC method described in the experimental section. The experiment was performed once for each ferrocifen.

Interfacial tension measurements (first method). Measurements of interfacial tension were performed using a drop tensiometer device (Tracker Teclis, Longessaigne, France). First, a 9 µL pendant drop of blank LNCs formulation, **P722**-LNCs formulation at 5.2 mg/g or **P769**-LNCs formulation at 5.2 mg/g, in contact with air, was generated with an Exmire microsyringe (Probablo, Paris, France). To keep the volume of the drop constant and so the surface area, piston movements of the syringe were controlled by a stepping motor. Interfacial tension, surface area and volume of the drop were obtained using the Laplace equation after analysis of the drop profile recorded in real time (1 measurement each 10 s) for 6 h using a video camera connected to a computer. All measurements were performed twice.

Determination of the molecular interactions for the gel formation. P769-LNCs at 17.2 mg/g was prepared using the phase inversion process. During the third cycle, when the temperature decreased and reached the PIT (78°C < PIT < 83°C), cold urea aqueous solutions (50, 100, 200 urea/**P769** mol/mol), NaCl solutions (50, 100, 200 NaCl/**P769** mol/mol), or ethanol-water mixtures (50, 100, 200 EtOH/**P769** mol/mol) were added, instead of cold water, to induce the irreversible shock to obtain LNCs. Formulations were stored at 4°C for one night. Gel viscoelastic properties were measured as explained in the experimental section. Elastic moduli G' and viscous moduli G'', were measured by varying the oscillation frequency (from 0.1 to 10 Hz), using a Kinexus® rheometer (Malvern Instruments S.A, United Kingdom). Values of G' and G'' were taken at 1 Hz. All these experiments were performed twice.

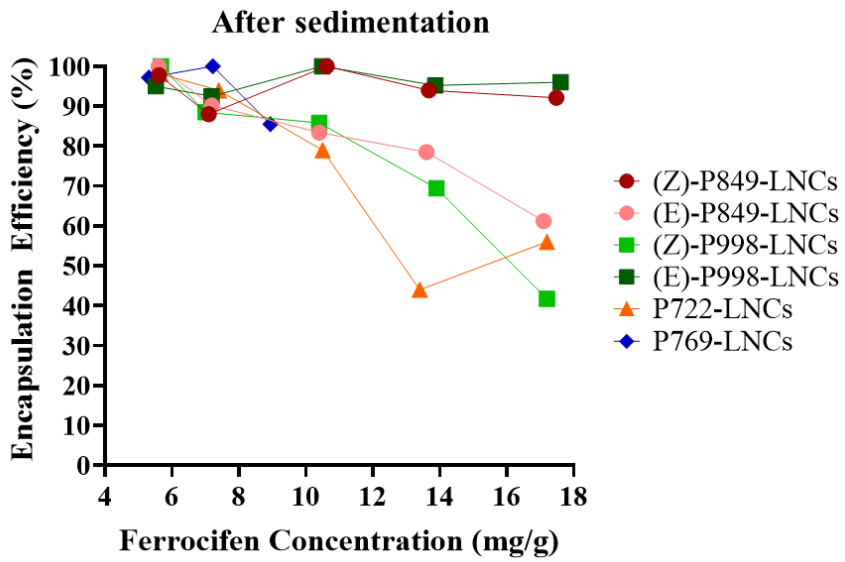

Figure S1: Encapsulation efficiency (E.E) (%) of succinimido-ferrocifen molecules in LNCs according to initial amounts of ferrocifens after sedimentation of unloaded ferrocifen. Ferrocifen concentration is expressed according to the weight of all lipophilic excipients (ferrocifen + Labrafac® WL 1349 + Kolliphor® HS 15 + Lipoïd S100) (n = 1).

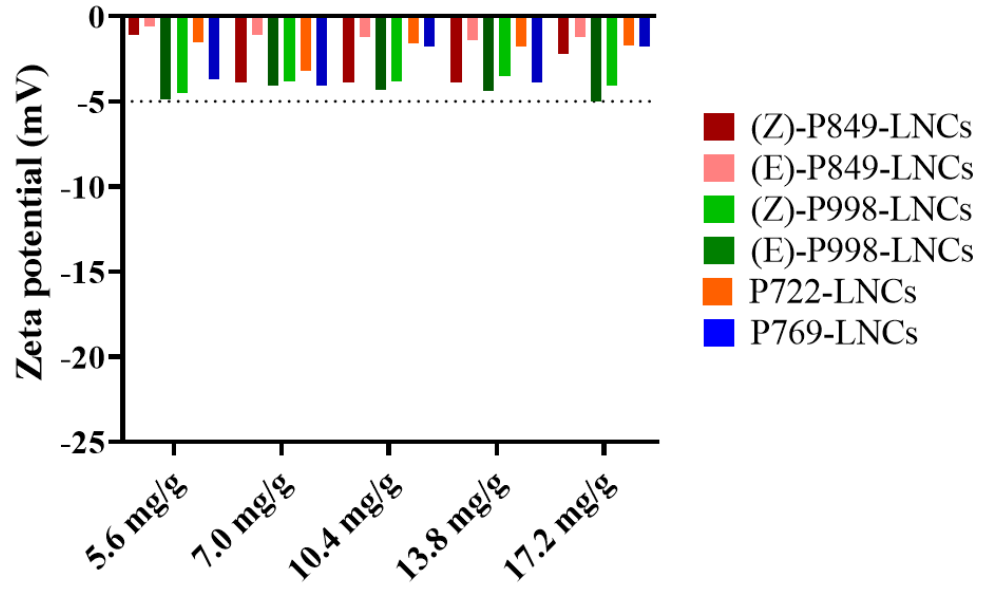

Figure S2: Zeta potential of ferrocifen lipid nanocapsules (LNCs) obtained by laser Doppler micro-electrophoresis technique. Results are the repetition of three measurements for each sample (n = 1).

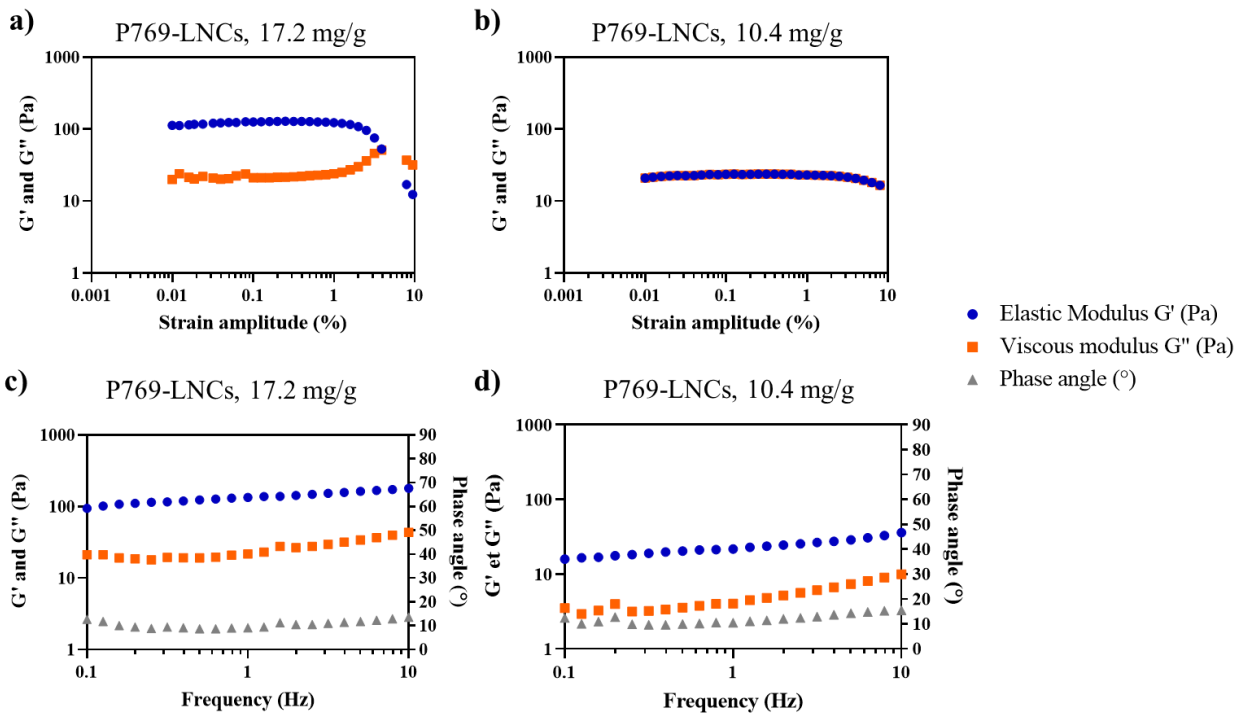

Figure S3: Mechanical properties of **P769**-LNC gel. a) Elastic G' and viscous G'' moduli measured during strain amplitude sweep at a constant oscillation frequency of 1 Hz, to determine the linear regime, for **P769**-LNCs at 17.2 mg/g ; b) Elastic G' and viscous G'' moduli measured during strain amplitude sweep at a constant oscillation frequency of 1 Hz, to determine the linear regime, for **P769**-LNCs at 10.4 mg/g ; c) Elastic G' and viscous G'' moduli measured during oscillatory frequency sweep at a constant strain amplitude of 0.1 % for **P769**-LNCs at 17.2 mg/g ; d) Elastic G' and viscous G'' moduli measured during oscillatory frequency sweep at a constant strain amplitude of 0.1 % for **P769**-LNCs at 10.4 mg/g.

Table S1: Rheological properties of the **P769**-LNC and **(E)-P998**-LNC gels (n = 3, mean ± SD).

Gel	P769 concentration (mg/g)	LNC concentration (LNC/mL)	Extrusion	G'/G''
P769-LNCs	10.4	$2.72x10^{15}$	No	7.88 ± 4.45
	13.8	$2.72x10^{15}$	No	4.91 ± 1.65
	17.2	$2.72x10^{15}$	No	5.37 ± 1.23
	17.2	$6.59x10^{14}$	No	4.17 ± 1.21
	17.2	$1.14x10^{15}$	No	4.95 ± 0.80
	17.2	$2.72x10^{15}$	No	5.37 ± 1.23
	17.2	$2.72x10^{15}$	18 G needle	4.90 ± 0.16
	17.2	$2.72x10^{15}$	26 G needle	3.49 ± 0.08
(E)-P998-LNCs	17.2	$2.72x10^{15}$	No	5.72 ± 2.02
	20.6	$2.72x10^{15}$	No	5.55 ± 0.61

	27.3	$2.72x10^{15}$	No	4.17 ± 0.83
	33.9	$2.72x10^{15}$	No	5.21 ± 0.70

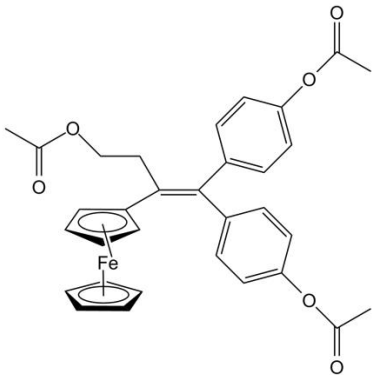

P996

Formulation	Diameter (nm)	PDI	Zeta potential (mV)
P996-LNCs, 17.2 mg/g	52.4	0.054	-6.0
P996-LNCs, 36.4 mg/g	53.0	0.058	-5.7

Figure S4: Molecular structure of **P996** and physico-chemical characterization of **P996**-LNCs at 17.2 mg/g and 36.4 mg/g. No gel was obtained at these concentrations as shown on the photo.

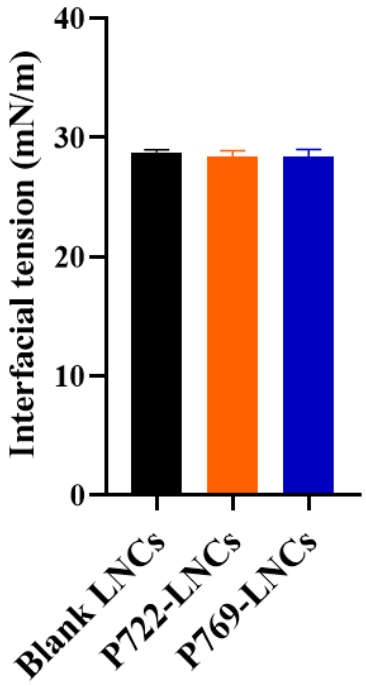

Figure S5: Interfacial tension measurement of a 9 µL LNC suspension drop, with or without ferrocifen, in contact with air, after 6 h of adsorption kinetics. Ferrocifen concentration was fixed at 5.2 mg/g of lipophilic compounds (n = 2, mean ± SD).

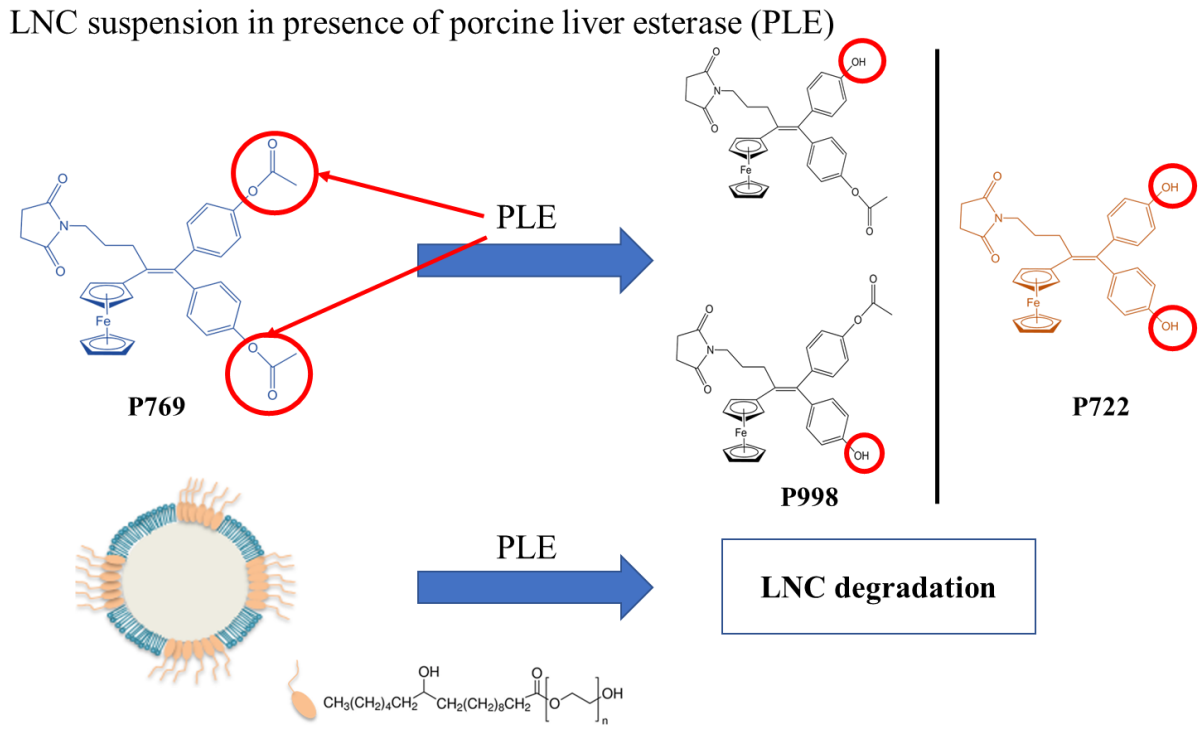

Figure S6: Schematic representation of the possible competitive hydrolysis by esterase between ferrocifen **P769** and polyethylene glycol hydroxystearate from the LNC shell.

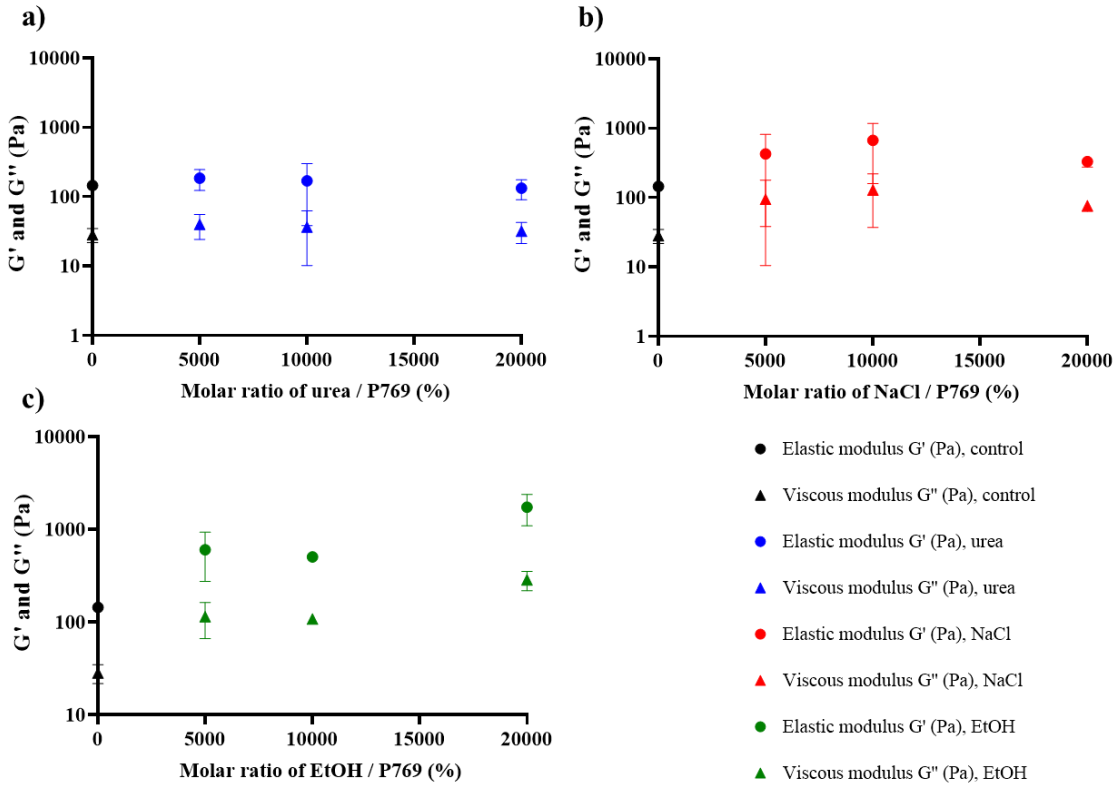

Figure S7: a) **P769**-LNC gel rheological behaviour (elastic G' and viscous G'' moduli), at 17.2 mg/g in **P769**, according to the molar ratio between urea and **P769**; b) **P769**-LNC gel rheological behaviour (elastic G' and viscous G'' moduli), at 17.2 mg/g in **P769**, according to the molar ratio between NaCl and **P769**; c) **P769**-LNC gel rheological behaviour (elastic G' and viscous G'' moduli), at 17.2 mg/g in **P769**, according to the molar ratio between EtOH and **P769** (n = 2, mean ± SD).

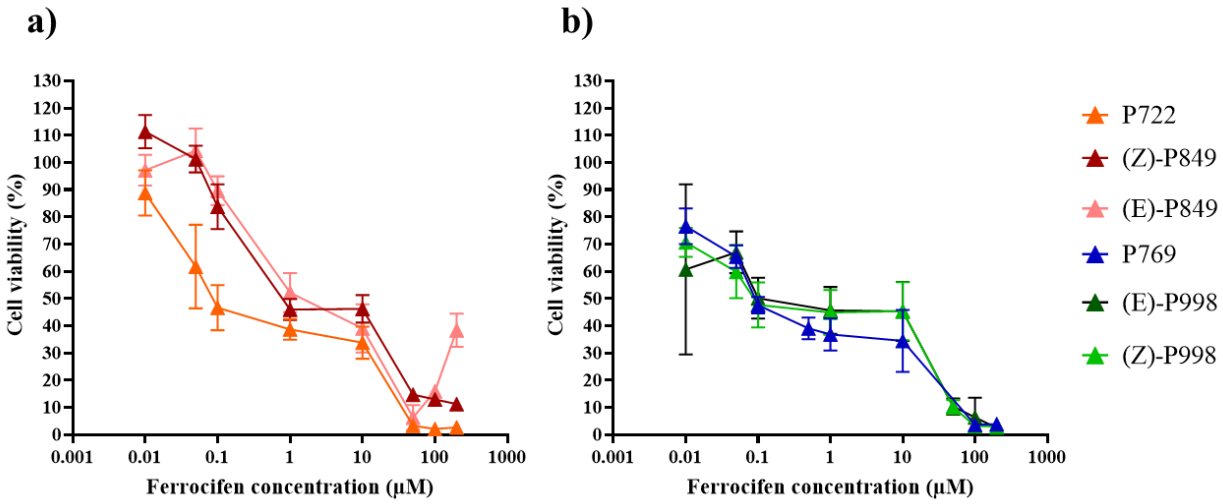

Figure S8: Cell viability of SKOV3 cells after 72 h of treatment with several concentrations of: a) **P722** (orange circle), **(Z)-P849** (dark red circle) and **(E)-P849** (pink circle); b) **P769** (dark blue circle), **(E)-P998** (dark green circle) and **(Z)-P998** (green circle) (3 < n < 4, mean ± SD).

The identification of *E* and *Z* isomers in these systems by NMR spectroscopy was based on the nuclear Overhauser effect (nOe), a phenomenon whereby nuclei proximate in space to each other exhibit peak enhancement; the effect diminishes rapidly with distance (having a $1/R^6$ dependence). In the two-dimensional version of this experiment (NOESY), off-diagonal cross-peaks reveal these specific interactions. In the monophenol **P849**, clear interactions are seen between protons in the ferrocenyl moiety and those in the unsubstituted phenyl ring, whereas protons in the phenol ring correlate with those in the propyl chain linked to the succinimido group; this unambiguously establishes the *E*-geometry such that the phenol is sited *cis* to the succinimido substituent and *trans* to the ferrocenyl sandwich unit.

In the monophenolic ester **P998**, each aryl ring is para-substituted giving rise to distinctive pairs of doublet proton resonances, only one of which clearly interacts with the propylsuccinimido protons. The distinction between the simple phenol ring and the one bearing the ester substituent rings was readily accomplished by direct comparison of the spectra of the diphenol **P722** and the diester **P769**. As shown in **Figure S11**, protons in the esterified rings are markedly deshielded relative to those of the diphenol. Hence, in the lowest spectral trace shown in Figure S10, the major product is the *E* isomer.

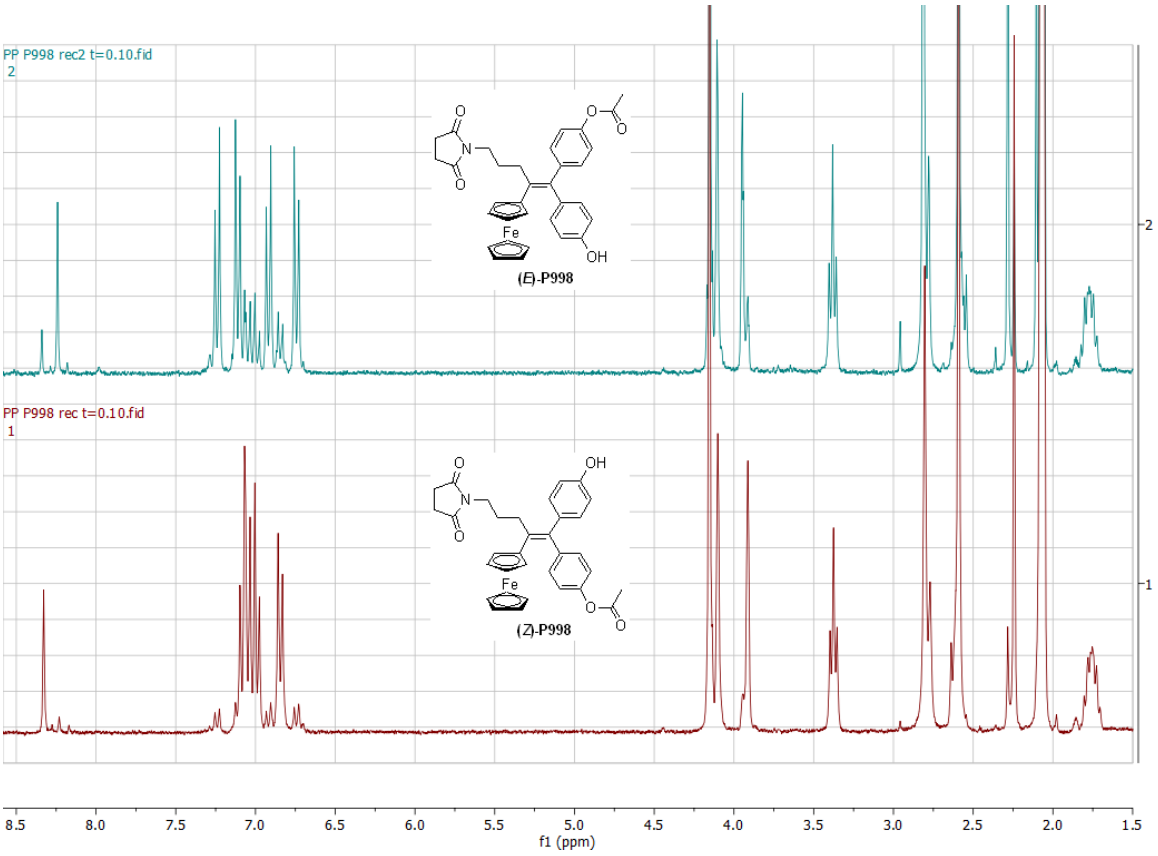

Figure S9: Monophenol ester **P998** after first recrystallization (lower trace, richer in *Z* isomer), and after concentration of the remaining solution followed by a second recrystallization (upper trace, richer in *E* isomer).

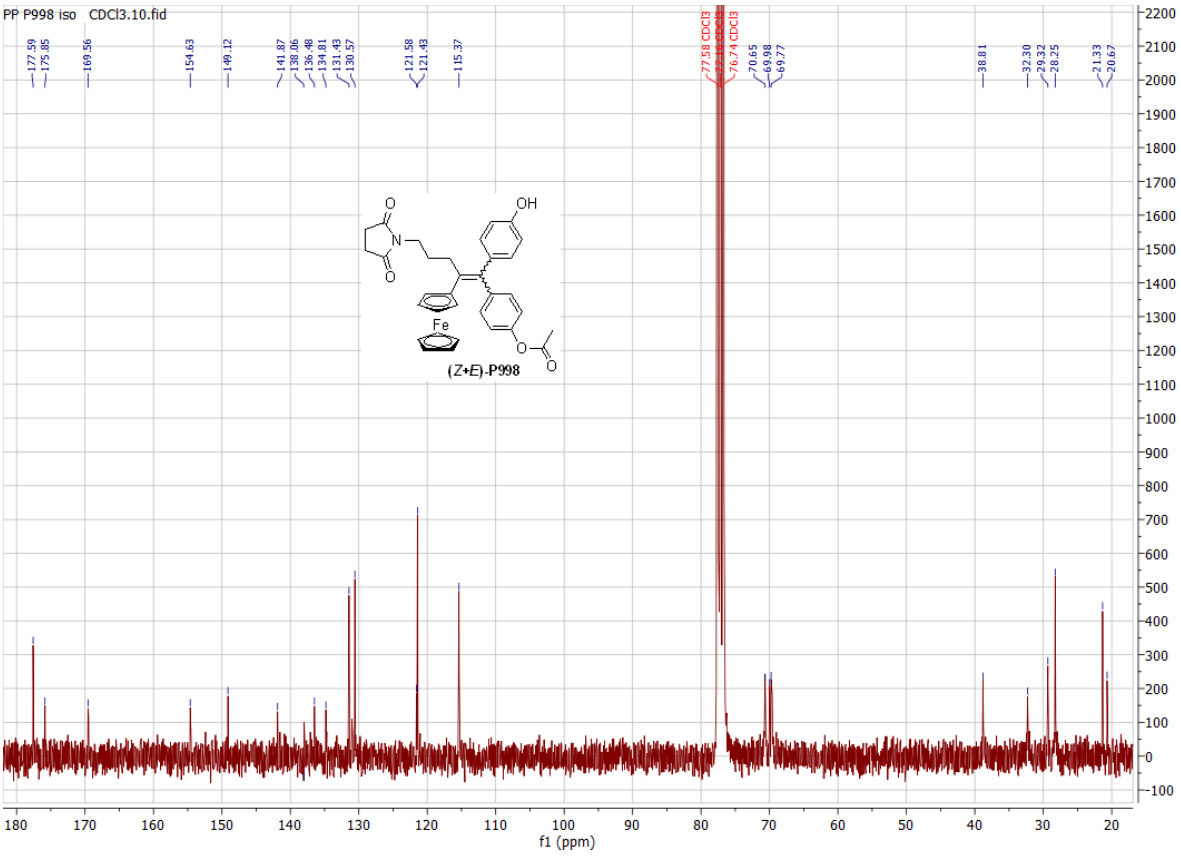

Figure S10: ^{13}C NMR spectra of **(*Z*+*E*)-P998** in $CDCl_3$, acquired on a Bruker 300 MHz spectrometer.

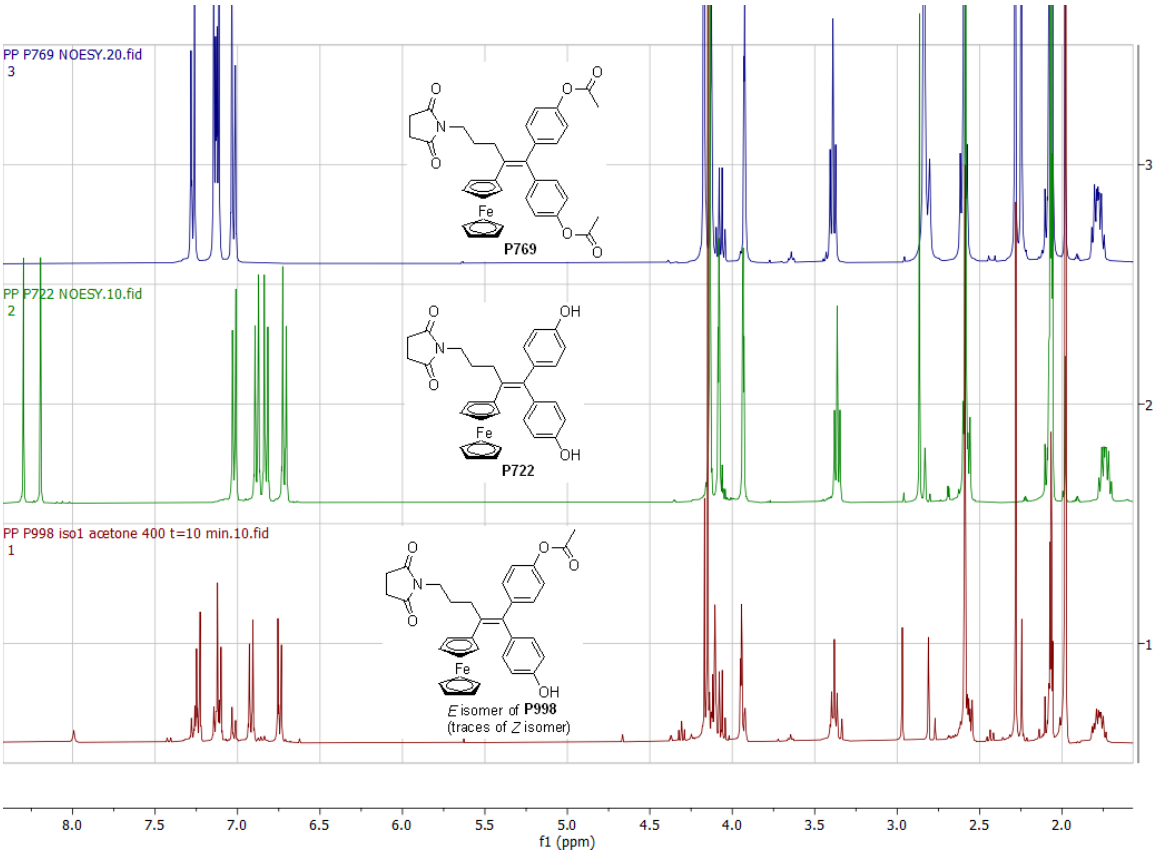

Figure S11: Superposition of **P769** (diester, upper trace), **P722** (diphenol, middle trace) and ***E*-P998** (mono-phenol-monoester, with traces of isomerization, lowest trace) to identify in **P998** where are C_6H_4-OH (right side of the aromatics, < 7.0 ppm) and C_6H_4-OAc (left side, >7.0 ppm), to help with the NOESY experiment.

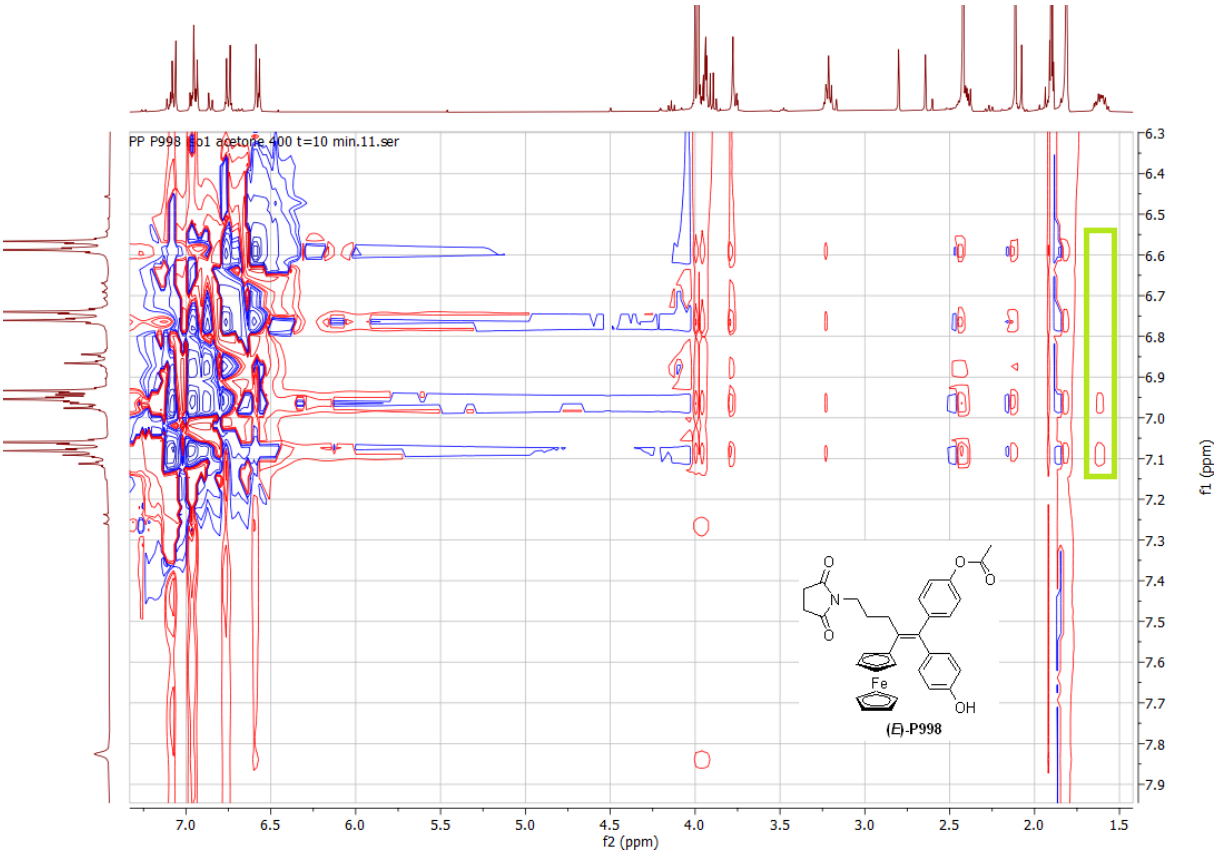

Figure S12: Zoom of the NOESY experiment carried out on isomer 1 of **P998**. The correlation of the protons of the CH_2 sited in the middle of the propyl chain (around 1.65 ppm) with the C_6H_4-OAc group, but not with the C_6H_4-OH group (green rectangle) reveals that its configuration is *E*.

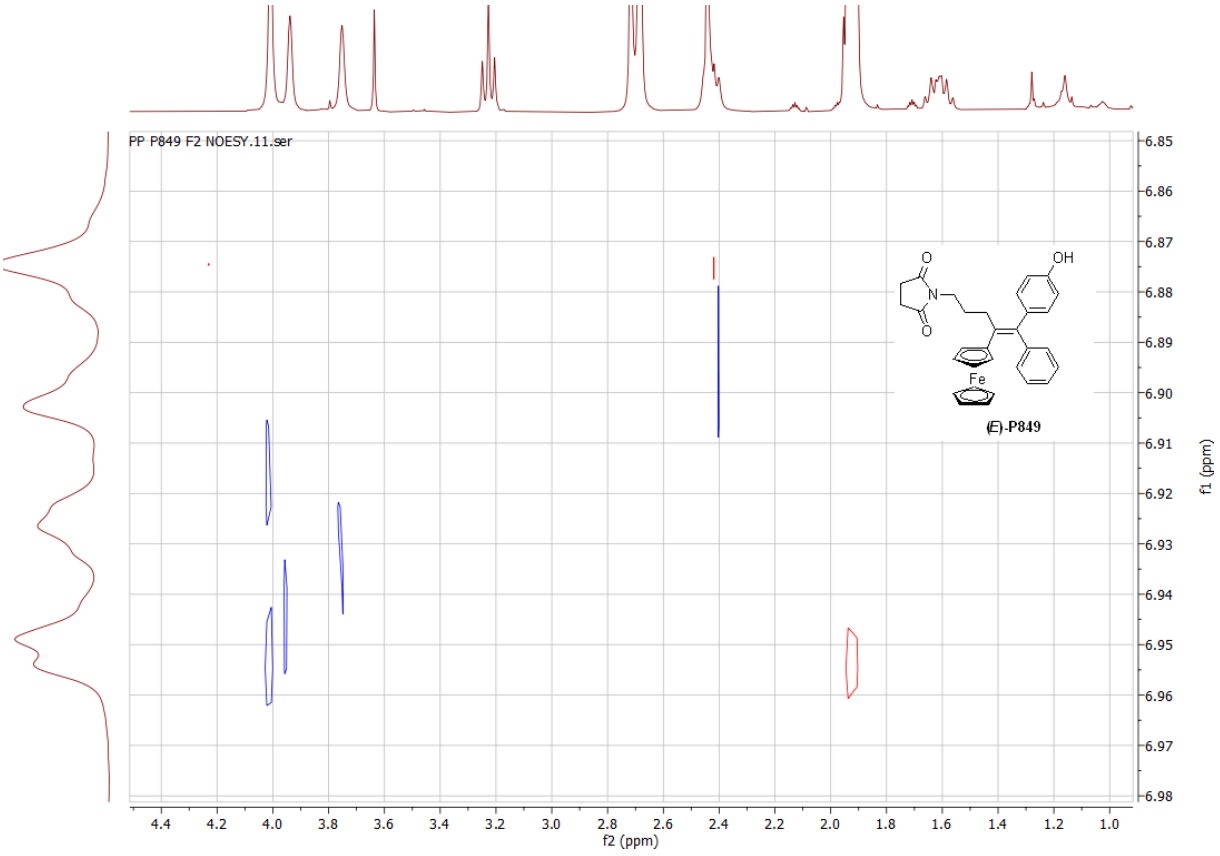

Figure S13: Zoom of the NOESY experiment carried out on isomer 2 of **P849**. The correlation of peak at 2.4 ppm (succinimide + CH_2 connected to the alkene double bond) and C_6H_4-OH reveals that this isomer is *E*. This is confirmed by the correlation of protons in the phenyl ring with those in the ferrocenyl group (Cp + C_5H_4). **P849** was already reported, but the *E* or *Z* configuration had not been established.

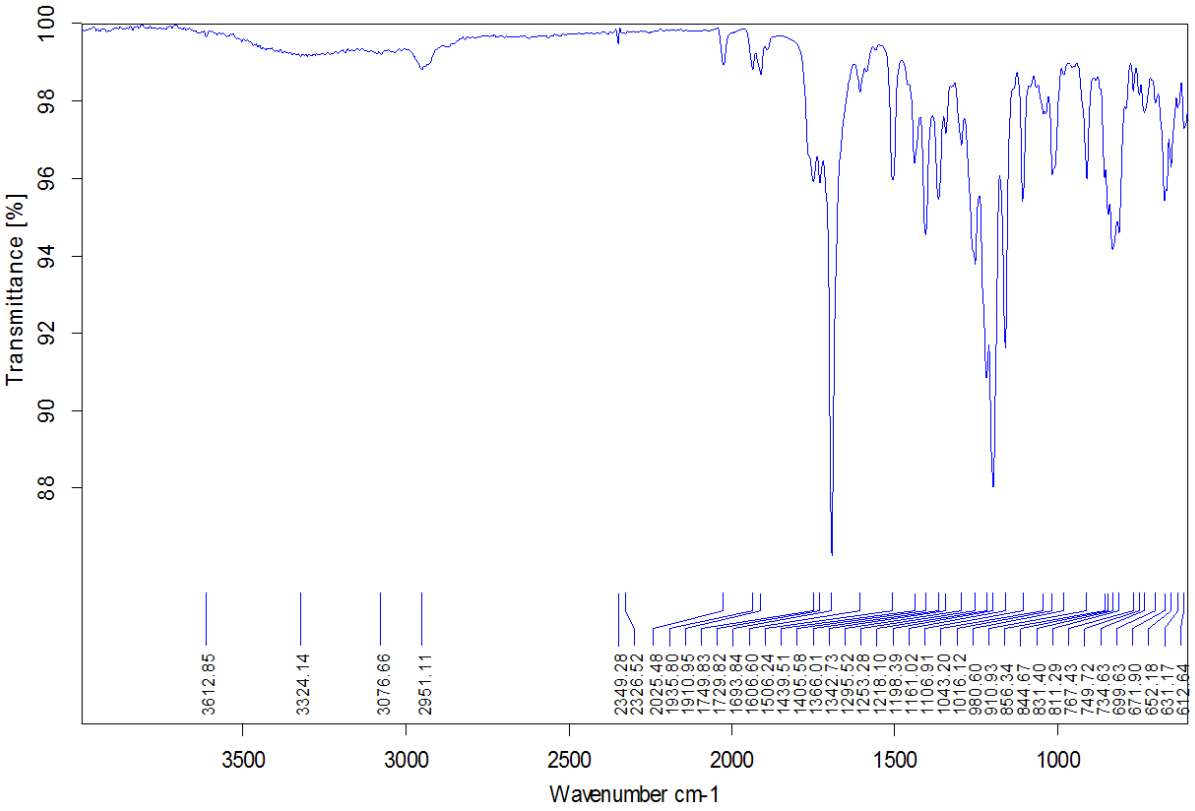

Figure S14: IR spectrum of **P998** (ATR).